



available at www.sciencedirect.com



journal homepage: www.elsevier.com/locate/jjcc



Review

Recent advances in coronary angiography

Yasumi Uchida (MD)*

Japan Foundation for Cardiovascular Research, 2-30-17, Narashinodai, Funabashi, Japan

Received 27 October 2010; accepted 29 October 2010
Available online 10 December 2010

KEYWORDS

Vulnerable coronary plaques;
Conventional angiography;
Dye-staining angiography;
Near-infrared fluorescence angiography;
Color fluorescence angiography

Summary Angioscopy enables macroscopic pathological diagnosis of cardiovascular diseases from the inside. This imaging modality has been intensively directed to characterizing vulnerable coronary plaques. Scoring of plaque color was developed, and based on prospective studies; dark yellow or glistening yellow plaques were proposed as vulnerable ones. Colorimetry apparatus was developed to assess the yellow color of the plaques quantitatively. The effects of lipid-lowering therapies on coronary plaques were confirmed by angioscopy. However, since observation is limited to surface color and morphology, pitfalls of this imaging technology became evident. Dye-staining angiography and near-infrared fluorescence angiography were developed for molecular imaging, and the latter method was successfully applied to patients. Color fluorescence angiography was also established for molecular and chemical basis characterization of vulnerable coronary plaques in both *in vitro* and *in vivo*. Drug-eluting stents (DES) reduce coronary restenosis significantly, however, late stent thrombosis (LST) occurs, which requires long-term antiplatelet therapy. Angioscopic grading of neointimal coverage of coronary stent struts was established, and it was revealed that neointimal formation is incomplete and prevalence of LST is higher in DES when compared to bare-metal stent. Many new stents were devised and they are now under experimental or clinical investigations to overcome the shortcomings of the stents that have been employed clinically. Endothelial cells are highly antithrombotic. Neoendothelial cell damage is considered to be caused by friction between the cells and stent struts due to the thin neointima between them that might act as a cushion. Therefore, development of a DES that causes an appropriate thickness (around 100 μm) of the neointima is a potential option with which to prevent neoendothelial cell damage and consequent LST while preventing restenosis.

© 2011 Japanese College of Cardiology. Published by Elsevier Ltd. All rights reserved.

Contents

| | |
|---|----|
| Introduction | 19 |
| Developmental history of coronary angiography | 19 |
| Vulnerable coronary plaques | 20 |

* Tel.: +81 47 462 2159; fax: +81 47 462 2159.
E-mail address: uchiy@ta2.so-net.ne.jp

| | |
|---|----|
| Detection of vulnerable coronary plaques by angiography | 20 |
| Classification of plaque color | 20 |
| Quantitative analysis of plaque color | 20 |
| Angioscopic identification of vulnerable plaques by surface color | 21 |
| Prediction of acute coronary syndromes by angiography | 21 |
| Relations of angioscopic images to those by intravascular ultrasonography (IVUS), optical coherence tomography (OCT) and computed tomography (CT)..... | 21 |
| Pitfalls of angiography in detecting vulnerable plaques | 21 |
| A vulnerable coronary plaque has a thin fibrous cap with a large lipid core beneath: A fact or story? | 22 |
| Pre-stage of erosion | 22 |
| Acute coronary syndromes without obvious coronary plaque disruption..... | 22 |
| Detection of vulnerable coronary plaques by new imaging modalities..... | 22 |
| Detection of vulnerable coronary plaques by near-infrared spectroscopy | 23 |
| Detection of vulnerable coronary plaques by near-infrared fluorescence angiography..... | 23 |
| Detection of vulnerable coronary plaques by color fluorescence angiography | 23 |
| Evaluation of progressiveness toward vulnerable plaques | 23 |
| Oxidized low-density lipoprotein imaging | 23 |
| Lysophosphatidylcholine imaging..... | 23 |
| Cholesterol and cholesteryl ester imaging | 24 |
| Macrophage imaging | 24 |
| Evaluation of stabilization and regression of vulnerable plaques by angiography | 24 |
| Lipid-lowering therapy..... | 24 |
| Molecular or cellular targeting therapy | 25 |
| Evaluation of neointimal coverage of coronary stents by angiography..... | 25 |
| Grading of neointimal coverage by angiography..... | 25 |
| Difference in neointimal coverage between bare-metal and drug-eluting stents | 25 |
| Late-stent thrombosis..... | 25 |
| Possible mechanisms of late-stent thrombosis and appropriate neointimal thickening to prevent restenosis, and neoendothelial cell damages and consequent late-stent thrombosis..... | 26 |
| Conclusion..... | 28 |
| References | 29 |

Introduction

Angioscopy enables macroscopic pathological diagnosis of cardiovascular diseases from the inside. This imaging modality has been intensively directed to characterizing vulnerable coronary plaques. Scoring of plaque color was developed, and based on prospective studies, dark yellow or glistening yellow plaques were proposed as vulnerable ones. Colorimetry apparatus was developed to assess the yellow color of the plaques quantitatively.

The effects of lipid-lowering therapies on coronary plaques were confirmed by angiography. However, since observation is limited to surface color and morphology, pitfalls of this imaging technology became evident.

Dye-staining angiography and near-infrared fluorescence angiography were developed for molecular imaging, and the latter method was successfully applied to patients. Color fluorescence angiography was also established for molecular and chemical basis characterization of vulnerable coronary plaques in both *in vitro* and *in vivo*.

Drug-eluting stents (DES) reduce coronary restenosis significantly, however, late stent thrombosis (LST) occurs, which requires long-term antiplatelet therapy. Mechanisms of LST were clarified considerably by angiography.

This article describes the past and present status of coronary angiography.

Developmental history of coronary angiography

On August 31, 1945, a big storm hit the Kanto district of Japan. Trains were stopped for several hours due to the storm and Tsutomu Uji, a surgeon from Tokyo University and Masanao Sugiura of Olympus Company happened to meet in the train. A concept of new endoscope was discussed, which could be the start of the development of endoscopy in Japan.

In December 1949, in collaboration with Masao Fukaomi and Minoru Maruyama, they developed a flexible gastroscope 12 mm in diameter with films and illumination source in the distal most tip. Anesthetized dogs were successfully examined with this endoscope.

Takeshi Sakamoto used this endoscope for the first time as a gastroscope. A flexible gastroscope thus developed has provided the basic structure for bronchoscopes, cystoscopes, etc.

Several years later, this gastroscope was replaced by a fiberscope which was more flexible and more easy to be manipulated. Fiberscopes have been widely applied to diagnosis and treatment not only of digestive tracts but also respiratory and urogenital tracts as an essential tool.

Although an endoscope was clinically applied to the heart during surgery by Allen in 1922 [1], many years elapsed until percutaneous transluminal coronary angiography was

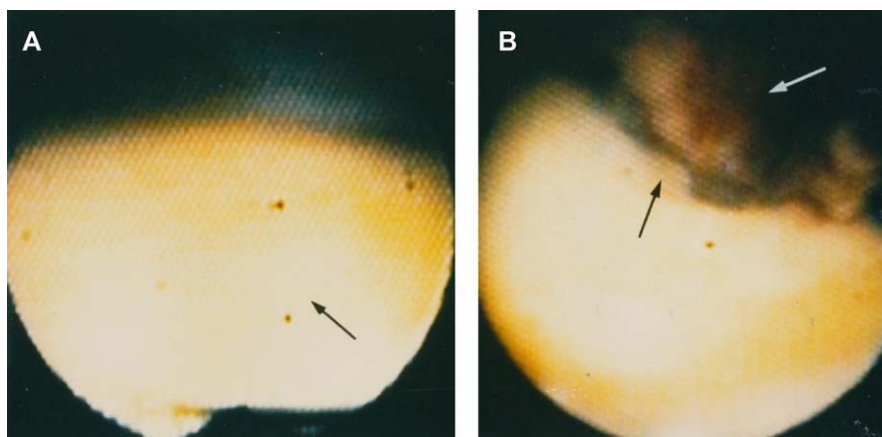


Figure 1 Angioscopic images of a coronary plaque before and after disruption. A 60-year-old male. A glistening yellow plaque in the proximal segment of the right coronary artery before (black arrow in A) and disruption of the identical plaque (black arrow in B) and thrombus formation (white arrow in B) observed 3-h after the onset of acute coronary syndrome. Reproduced from Uchida et al. [15], with permission.

performed. This was due to the difficulty in the displacement of blood in the artery and the need for more flexible and thinner endoscope.

With anticipation for clinical application, we (the author and employees of Olympus Co) began to develop a new fiberoptic endoscope for coronary use in 1976. Thrombosis and thrombolysis in the removed human coronary artery and the changes induced by balloon angioplasty were successfully observed by this endoscope in 1986 [2].

Meanwhile, Spears observed coronary ostia by the use of a bronchoscope [3]. Also, coronary arterial changes were observed mainly intraoperatively by Litvack [4].

Using fiberoptic endoscopes specially designed for coronary use, the author observed percutaneously from proximal to distal coronary segments in patients with ischemic heart disease (1984, 1987) [5]. Observation of plaque disruption and thrombi in acute coronary syndromes (ACS) was performed by Hoeler [6]. Evaluation of coronary interventions by POBA was performed by the author (1989) [7,8]. Coronary intervention by laser was evaluated by the author (1987), Nakamura [9], and evaluation of coronary interventions by stent by Ueda [10]. Stent and cutting balloon were studied by many investigators. Application of percutaneous coronary angiography was extended to diagnosis of Kawasaki disease by Ishikawa [11].

Thus, percutaneous angiography is now routinely performed for examinations of underlying mechanisms of ACS [12], for selection of therapeutic modalities, for evaluation of medical [13], interventional [14], and surgical therapies and for prediction of ACS [15].

Vulnerable coronary plaques

It is still not predictable, in whom, when, where and during what she (he) is doing, ACS occur. If they become predictable, it is a great gospel for mankind. Many workers have devoted time to characterize vulnerable coronary plaques that trigger these fatal syndromes. However, characterization of vulnerable coronary plaques is still not established.

Vulnerability has two aspects of meaning; one is the fragile plaques that are easily disrupted by mechanical stimuli and another is the plaques rapidly progressing toward fragile ones by inflammatory or metabolic processes. In clinical situations, the former are usually considered as vulnerable ones.

Detection of vulnerable coronary plaques by angiography

Angiography has contributed to understanding the underlying mechanisms of ACS.

It was found that thrombus formation on the disrupted yellow coronary plaques is the typical causative mechanism of ACS in the majority of patients [4]. Therefore, a certain group of yellow plaques has been considered as vulnerable to disruption.

Fig. 1 demonstrates angioscopic images of a yellow plaque before and immediately after the onset of ACS (ST-elevation myocardial infarction). Disruption of the identical plaque and thrombus formation on it were evident after the onset of attack [15].

Classification of plaque color

Scoring of vulnerability by surface color was made; namely white, light yellow, yellow, and dark yellow as 0, 1, 2, and 3 respectively; or white, light yellow, yellow, and glistening yellow plaques as 0, 1, 2, and 3, respectively [16–18] (Fig. 2).

Since dark yellow and glistening yellow plaques often have thin fibrous cap with lipid pool beneath by histology, intravascular ultrasonography (IVUS) or optical coherence tomography (OCT), they are proposed as vulnerable ones.

Quantitative analysis of plaque color

Angioscopic color assessment of plaques is influenced by light irradiated onto them. Furthermore, yellow color

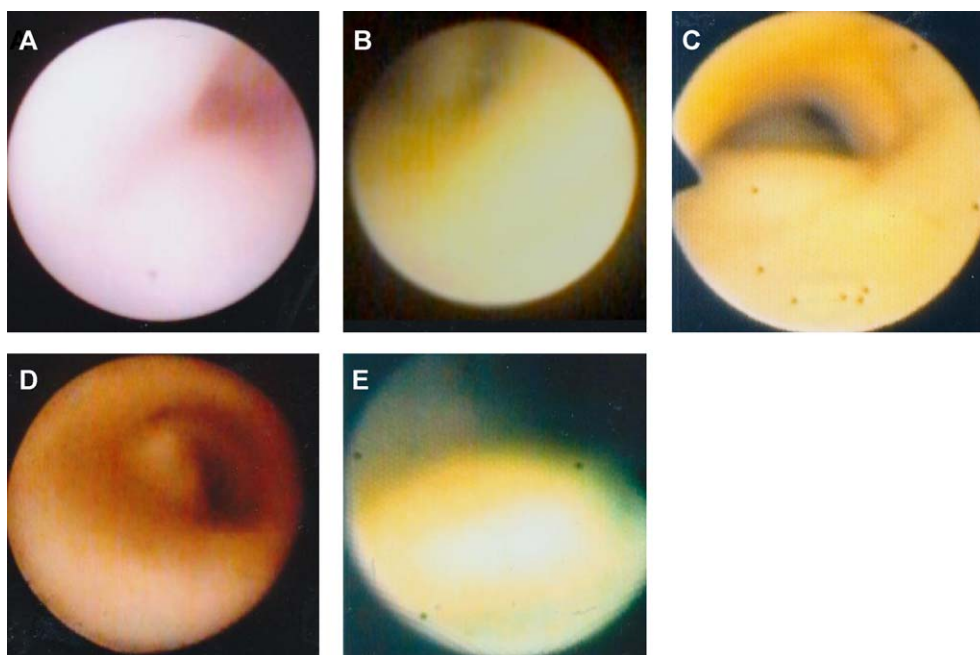


Figure 2 Angioscopic classification of coronary plaques. From A to E: white, light yellow, yellow, dark yellow, and glistening yellow plaques, respectively.

grading is often different from observer to observer. Therefore, intra- and interobserver observation system has been employed for color grading.

In order to avoid this rather subjective grading, a quantitative color analysis was attempted. Ishibashi et al. and Okada et al. developed a colorimetry apparatus for quantitative assessment of yellow color of the plaques, and they found that the plaques with high yellow color are vulnerable to thrombosis [19,20].

Angioscopic identification of vulnerable plaques by surface color

Although scoring of vulnerability by depth of yellow color is one approach for characterization of vulnerable plaques, relationships between depth of yellow color and histological vulnerability remain unclear. It was reported that yellow color of human coronary plaques is determined by deposition of β -carotene, and in addition to its concentration, its deposition with cholesteryl esters increases depth of yellow color [21]. Therefore, relationships between histological changes and molecular imaging of lipids should be examined for more specific diagnosis of vulnerable coronary plaques.

Since angioscopic observation is limited to surface color and morphology, the histological and molecular changes inside the plaque are beyond the scope of this imaging technology.

Prediction of acute coronary syndromes by angioscopy

It was reported that the glistening yellow plaques are prone to disrupt and ACS more frequently develop in patients having this type of plaque and the changes in the identical

plaques before and immediately after onset of ACS were observed by angioscopy. It was revealed that ACS developed in 3.3% of white plaque group, 7.6% of non-glistening yellow plaque group, and 68.4% of glistening yellow plaque group [15].

Ohtani et al. followed up 552 patients by angioscopy for 57.3 months. ACS events occurred in 7.1%. Patients with number of yellow plaques ≥ 2 and ≥ 5 had 2.2 and 3.8-fold higher event rates, respectively than those with number of yellow plaques 0 or 1 [22].

Relations of angioscopic images to those by intravascular ultrasonography (IVUS), optical coherence tomography (OCT) and computed tomography (CT)

Coronary plaques were analyzed by angioscopy and OCT in combination by Takano et al. They observed an inverse relation between color grade and fibrous cap thickness [23]. Komatsu et al. classified coronary plaques by multi-detector row computed tomography into soft, intermediate, and calcified plaques, and he found good correlation between soft plaque and angioscopic yellow plaque [24].

Pitfalls of angioscopy in detecting vulnerable plaques

The yellow color of the plaques is mainly caused by β -carotene which coexists with lipids in the vascular wall, and therefore it is an indirect marker of vulnerability.

All prospective studies indicate that yellow plaques are more prone to disruption than white plaques, but do not indicate that all yellow plaques become disrupted.

Table 1 Histological classification of coronary plaques based on distribution of lipids, calcium, collagen fibers, and macrophage-foam cells.

| Angioscopy | Histology |
|-------------------------------|--|
| | Superficial lipid deposition group CF-dense subtype CF-loose subtype CF-scanty subtype |
| Glistening yellow plaques | Diffuse lipid deposition group Non-NC type CF-dense subtype CF-loose subtype CF-scanty subtype NC type |
| Non-glistening yellow plaques | Non-calcified cap type CF-dense, CF-loose, CF-scanty subtypes Calcified cap type CF-dense, CF-loose, CF-scanty subtypes |
| White plaques | Non-lipid deposition group Regular subtype Jelly-like subtype Calcified cap subtype |

The limited incidence of ACS in patients having yellow plaques (even in high yellow plaque patients and multiple yellow plaque patients) suggests the existence of both stable and vulnerable plaques in the yellow plaque group. ACS developed, although at a lower incidence (4%), in patients in whom white plaques but not yellow plaques were detected. Furthermore, disrupted white coronary plaques were observed in a prospective study [15]. This finding suggests the existence of vulnerable white plaques.

Coronary arteries are muscular arteries, and therefore coronary arteries and the plaques therein are protected against disruption by normal collagen fibers (CFs). During plaque growth, CFs degenerate, are disrupted, and finally destroyed.

Occlusive thrombosis occurs on the damaged (irrespective of erosion, ulcer, or lipid pool disruption) superficial layers of the coronary plaques, and results in ACS. Therefore, demonstrating the lack of normal CFs together with lipids and macrophages in the superficial layers of the plaques is an essential requisite for the detection of vulnerable plaques. However, detailed examinations of the relationships between angioscopic color images and the distribution of CFs are currently lacking.

In our study, white and yellow plaques were histologically classified into three and seven subtypes, respectively (Table 1). CF-loose-to-scanty subtype of superficial lipid deposition group, CF-loose-to-scanty cap subtype of lipid pool (necrotic core) type, and calcified cap subtype of lipid pool type in diffuse lipid deposition group of yellow plaques were considered to be vulnerable. These subtypes exhibited glistening yellow color, suggesting this color is a marker of vulnerable plaques [25,26].

A vulnerable coronary plaque has a thin fibrous cap with a large lipid core beneath: A fact or story?

A plaque having a thin fibroatheromatous cap with a large lipid core beneath has been believed to be vulnerable. Based on this hypothesis, intensive clinical studies have been carried out to investigate this type of plaque using IVUS and OCT. However, ACS do not necessarily develop in patients having a thin capped lipid core. Therefore, the thickness of the cap was measured in a pathohistological study. However, there were no significant differences in cap thickness among the CF-dense (histologically stable), CF-loose-to-scanty (histologically vulnerable), and calcified cap subtypes (histologically vulnerable), indicating that cap thickness did not necessarily represent vulnerability [25].

Whether the hypothesis “the vulnerable plaque has a thin fibrous cap with a large lipid core beneath” is a fact or story should be settled.

Pre-stage of erosion

Plaque erosion is observed in around 25% of patients with ACS, and sudden death not infrequently occurs in this group of patients [27,28]. Although erosion can be detected by angioscopy and OCT, what kind of images represents the pre-stage of erosion by these and other imaging tools had been unclear. We conceived that jelly-like type in white plaque, CF-scanty subtype of superficial lipid deposition group, and calcified cap subtype of yellow plaques were a pre-stage of erosion.

Acute coronary syndromes without obvious coronary plaque disruption

There are patients with ACS in whom disrupted coronary plaques are not detectable. Persistent coronary spasm or accidental coronary thromboembolism has been proposed as the causative mechanisms, however without definite evidence.

Fluffy (frosty glass-like) luminal surface of a non-stenotic coronary segment was observed in a certain group of patients with ACS (Fig. 3). The same luminal changes were reproduced in animals when blood was perfused after endothelial damages. Attachment of fibrin threads and platelets on the damaged endothelial cells was detected by histology, suggesting residual thrombus after autolysis. The same mechanisms may participate in patients with ACS without significant coronary stenosis, or without demonstrable plaque disruption. However, the genesis of endothelial damage remains to be elucidated [29]. Extensive endothelial cell apoptosis induced through catecholamine- β -adrenoceptor-caspase pathway [30] may play a role in this phenomenon.

Detection of vulnerable coronary plaques by new imaging modalities

Thus, limitation of conventional angioscopy using white light in detecting vulnerable plaques became evident. Therefore, the following imaging tools were developed for more objective diagnosis of vulnerable plaques.

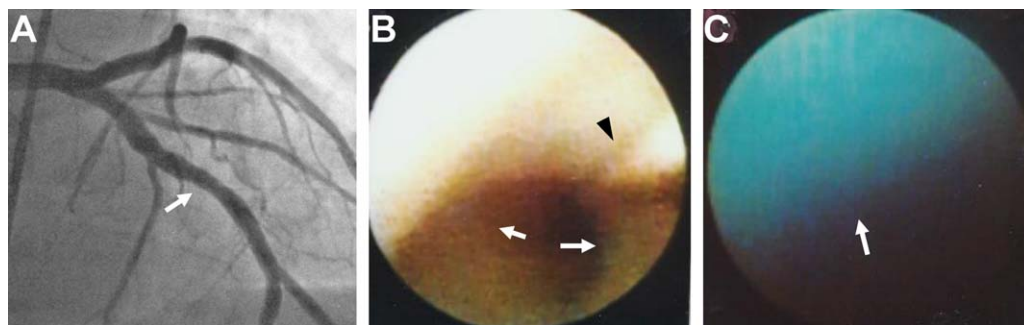


Figure 3 Fluffy coronary luminal surface. A 51-year-old female with unstable angina (UA). (A) Angiogram of the left coronary artery. The middle segment of the left anterior descending artery observed by angiography is shown by the arrow. The margin of the segment was irregular (arrow). (B) Angioscopic image of the same segment. The entire circumference of the luminal surface was fluffy (diffuse type) and white (arrows). Arrowhead, guidewire. (C) The fluffy surface was diffusely stained blue with Evans blue (arrow).

Reproduced from Uchida et al. [29] with permission.

Detection of vulnerable coronary plaques by near-infrared spectroscopy

Discrimination of cholesterol and cholesteryl esters in the excised human plaques by near-infrared spectroscopy (NIRS) *in vitro* was performed by Weinmann and Waxman [31,32]. This method is also applicable for detection of collagens, low-density lipoprotein, etc. This method has a potential use for molecular analysis of vulnerable plaques.

Detection of vulnerable coronary plaques by near-infrared fluorescence angiography

Two-dimensional imaging of cholesterol and cholesteryl esters within human coronary plaques was accomplished by near-infrared fluorescence angiography (NIRFA). The plaques in human coronary plaques both *in vitro* and *in vivo* were classified into NIRF absent, homogenous, doughnut-shaped, and spotty types. Histological examinations showed that these image patterns were determined mainly by β -carotene-conjugated cholesterol, cholesteryl esters, and calcium, and the latter two types were considered vulnerable [33] (Fig. 4).

Detection of vulnerable coronary plaques by color fluorescence angiography

Fluorescence of excised human coronary plaques was examined by color fluorescence angiography (CFA) using a 345 nm band-pass filter (BPF) and a 420 nm band-absorption filter (BAF).

Coronary plaques exhibited blue, green, white-to-light blue, or yellow-to-orange fluorescence. Fluorescence microscopic studies revealed that collagen subtypes, cholesterol, cholesteryl esters, calcium, and β -carotene determine the fluorescence color of the plaques. Histological examinations revealed dense CFs without lipids in blue plaques; dense CFs and lipids in green plaques; meager CFs and abundant lipids in white-to-light blue plaques; and the absence of CFs and deposition of lipids, calcium, and macrophage foam cells in the thin fibrous cap in yellow-to-orange plaques, indicat-

ing that the yellow-to-orange plaques were most vulnerable [34] (Figs. 5 and 6).

Evaluation of progressiveness toward vulnerable plaques

Based upon the knowledge about the pathophysiology of atherosclerosis, *in vitro* and *in vivo* and clinical trials have been performed using different tracers for plaque imaging studies, including radioactive-labeled lipoproteins, components of the coagulation system, cytokines, mediators of the metalloproteinase system, cell adhesion receptors, and even whole cells [26], or antibodies of the above-mentioned substances.

Oxidized low-density lipoprotein imaging

Oxidized low-density lipoprotein (OxLDL) plays a key role in the initiation, progression, and destabilization of atherosclerotic plaques [35,36].

Therefore, if oxLDL is visualized *in vivo*, the fate (progressiveness) of plaques can be prospected and the effects on them of medical and interventional therapies can be more objectively evaluated.

In the presence of Evans blue dye, oxLDL exhibited violet and brown fluorescence by exciting at 345 nm and emitted at 420 nm (A-imaging) and by exciting at 470 nm and emitting at 515 nm (B-imaging), respectively. This combination of fluorescence color was not observed in the other major substances composing atherosclerotic plaques. This combination of fluorescence was observed not only in yellow but also in white plaques of excised human coronary artery. Moreover, fluorescence characteristics of oxLDL in the coronary plaques were successfully visualized in patients [34] (Fig. 7).

Lysophosphatidylcholine imaging

Lysophosphatidylcholine (LPC) is a pro-inflammatory substance, and it is the major bioactive phospholipid component of oxLDL and plays a critical role in the atherogenic activity of oxLDL [37].

The fluorescence characteristic of LPC in excised human coronary plaques was investigated by color fluorescence

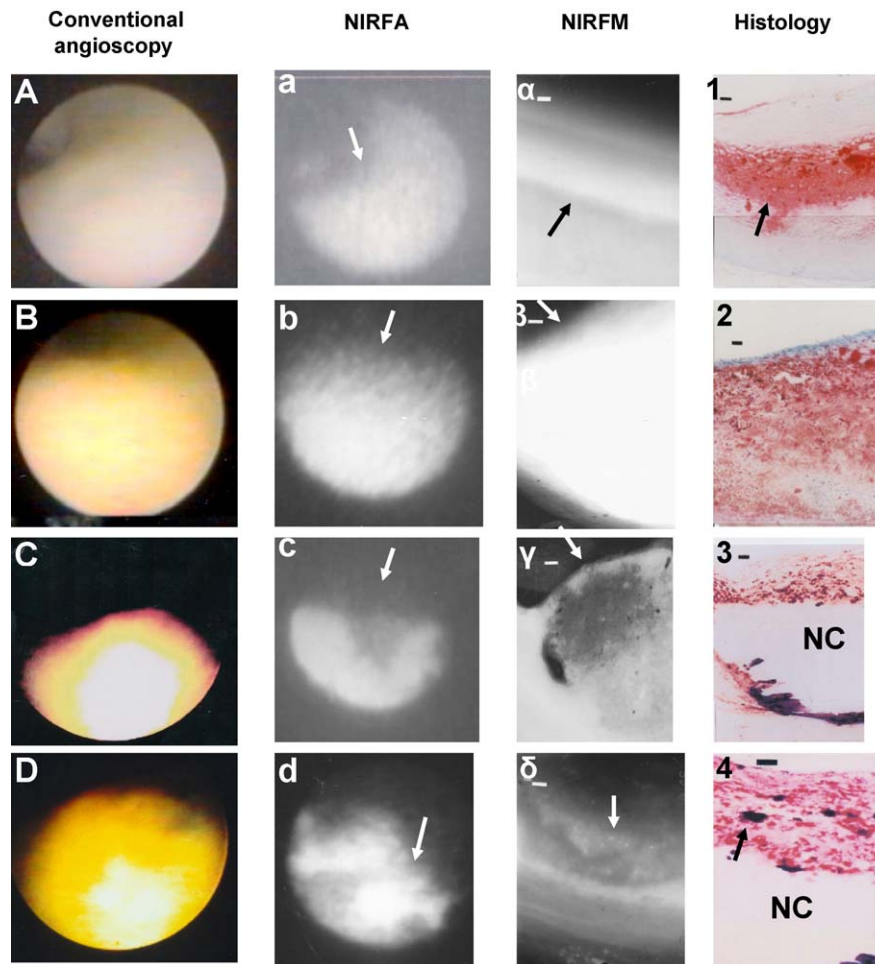


Figure 4 Relationships among conventional angioscopic, near-infrared fluorescence angiography (NIRFA), and near-infrared fluorescence microscopy (NIRFM) scanned images and histological changes in excised human coronary plaques. From A to D: the images of coronary plaques by conventional angioscopy. From a to d: corresponding NIRFA images of the same plaques. From α to δ : corresponding NIRFM scanned images of the cut wall surface of the same specimens. From 1 to 4: corresponding histological images after staining with Oil Red-O and methylene blue. Red and black portions indicate lipids and calcium, respectively. Horizontal bar at the left upper corner of each panel: 100 μm . A: a white plaque. From B to D: yellow plaques. a and b: homogenous type. Arrows: homogenous near-infrared fluorescence (NIRF); c: doughnut-shaped type. Arrow: NIRF absent portion surrounded by strong NIRF region; d: spotty type. Arrow: spots. α and β : homogenous NIRF (arrows); γ : necrotic core lacking NIRF (arrow) surrounded by strong NIRF region; δ : fibrous cap with strong NIRF spots (arrow). 1: homogenous deposition of lipids deep in the plaque (arrow); 2: lipid deposition in entire plaque; 3: lipid-deposited fibrous cap with a necrotic core (NC) below; 4: calcium particles distributed within a lipid-laden fibrous cap. Red: lipids. Black: calcium compounds (arrow). Horizontal bar: 100 μm . Reproduced from Uchida et al. [39], with permission

angioscopy using Trypan blue dye (TB) as an indicator. In the presence of TB, LPC exhibited a red fluorescence at A- and B-imaging. This red fluorescence at A- and B-imaging was observed in human coronary plaques [38].

Cholesterol and cholesteryl ester imaging

Garg and Waxman succeeded in *in vivo* imaging of cholesterol and cholesteryl esters by spectroscopy [32]. The present author succeeded in two-dimensional imaging of cholesterol and cholesteryl esters within the coronary plaques using NIRFA in patients [39] (Fig. 8).

Macrophage imaging

Macrophages play an important role in plaque progression. Discrimination of macrophages and foam cells is difficult

even by microscopy. Their imaging by angioscopy is still not successful. By imaging cells and molecules, vulnerable plaques can be characterized on a cellular or molecular basis.

Evaluation of stabilization and regression of vulnerable plaques by angioscopy

Lipid-lowering therapy

Effects of lipid-lowering therapy using fibrates or statins on coronary plaques were evaluated by several workers, and reduction of yellow color grade was observed as shown in Fig. 9 [13,40,41]. However, the changes in yellow plaque color induced by these agents were different among the plaques even in a given patient [13].

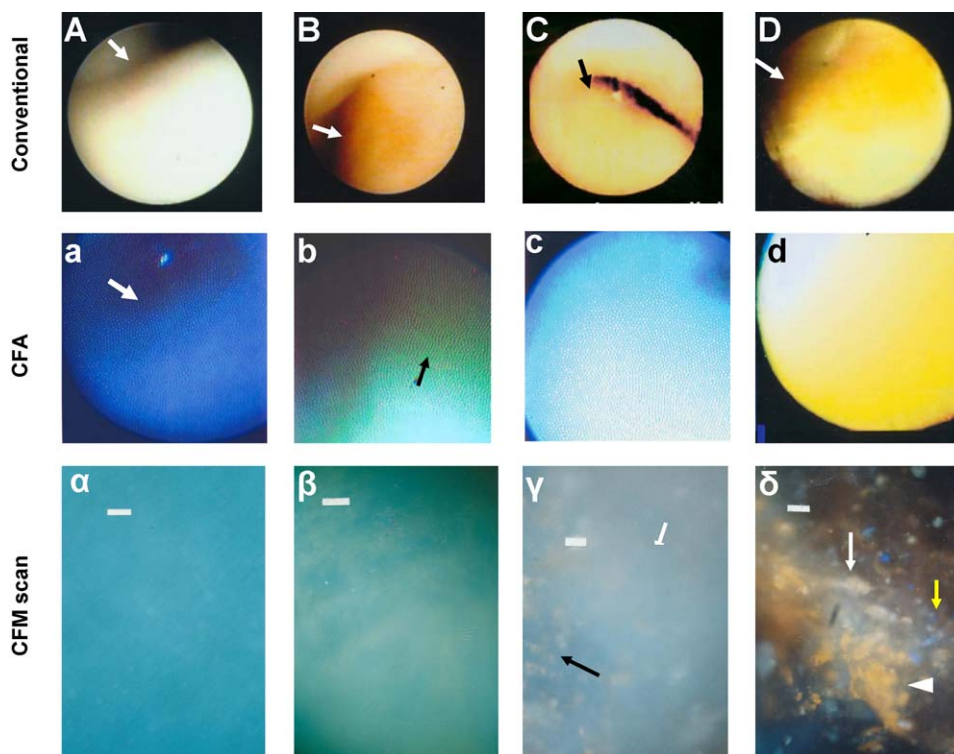


Figure 5 Relationships between images produced by conventional angiography, color fluorescence angiography (CFA) and color fluorescence microscopy (CFM) scanning. From A to D: conventional angiographic images of coronary plaques. From a to d: corresponding CFA images using "A" imaging. From α to δ : corresponding CFM scanned images using "A" imaging. Horizontal bar: 100 μm . A: a white plaque observed during conventional angiography (arrow) exhibited blue fluorescence by CFA (arrow in a) and CFM scan (α). B: a yellow plaque observed during conventional angiography (arrow) exhibited green fluorescence seen during CFA (arrow in b) and CFM scan (arrow in β). C: a yellow plaque observed during conventional angiography (arrow) exhibited white-to-light blue fluorescence seen during CFA (c) and deposition of yellow substances in the white-to-light blue area (arrow in γ). D: a yellow plaque observed during conventional angiography (arrow) exhibited yellow fluorescence observed during CFA (d) and deposition of orange (white arrowhead), white (white arrow) and blue (yellow arrow) substances in the area of no fluorescence by CFM scanning. Reproduced from Uchida et al. [34], with permission.

Molecular or cellular targeting therapy

Targeting therapy of oxLDL, metalloproteinases, or macrophages may be a promising option for stabilization and regression of vulnerable plaques. Although invasive, fluorescence angiography may be a promising imaging modality for direct evaluation of molecular or cellular targeting therapy of atherosclerotic plaques.

Evaluation of neointimal coverage of coronary stents by angiography

Neointima formation on stent struts is essential for vascular wound healing process. Drug-eluting stents (DES) inhibit the mobilization and differentiation of progenitor cells of endothelial cells and smooth muscle cells, and thus not only inhibit restenosis but also impair neointima formation, which may lead to stent thrombosis.

DES have reduced restenosis significantly, but their shortcomings became evident, namely insufficient stent strut coverage by neointima, and consequent late-stent thrombosis (LST) or very LST, and consequent ACS which can occur on termination of anti-thrombotic therapy. This is a typical example of "a new therapeutic modality that has a new complication".

Coronary angiography contributed greatly in clarifying mechanisms of neointimal coverage of stent struts and LST as follows:

Grading of neointimal coverage by angiography

The thickness of the neointima on the stent struts can be assessed by angiography based on whether or not the stent struts can be seen through the neointima.

Higo et al. and Oyabu et al. classified neointimal coverage by angiography into: grade 0, not covered; grade 1, covered by a thin layer; and grade 2, buried under neointima [42,43].

Difference in neointimal coverage between bare-metal and drug-eluting stents

Although restenosis rates have been markedly reduced by DES, it became evident that stent strut coverage by neointima was incomplete or much delayed in cases of DES when compared with bare-metal stents (BMS) [43–45]. It was also clarified that neointimal coverage is different among DES [46].

Late-stent thrombosis

Fig. 10 shows an example of occlusive LST. LST occurs in both BMS and DES. The prevalence was significantly higher in the

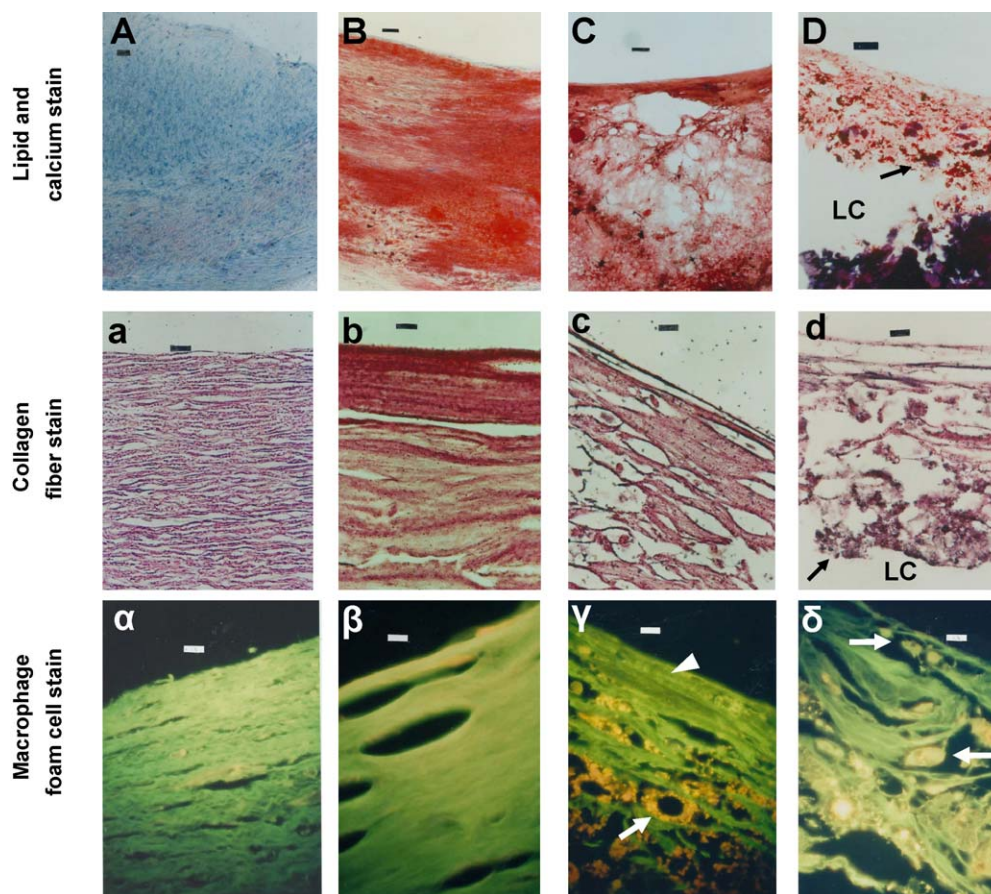


Figure 6 Lipids, calcium compounds, collagen fibers (CFs), and macrophage foam cells in the same plaques as those shown in Fig. 5. From A to D: microscopic images after Oil-red O and methylene blue staining obtained from the same plaques in A to D in Fig. 5, respectively. Red: lipids. Black: calcium. LC: lipid core. Horizontal bar: 100 μm . From a to d: CFs stained by silver staining. No normal CFs in d. Arrow in d: plaque debris. Horizontal bar: 20 μm . From α to δ : images of ceramide in macrophage foam cells obtained by "B" imaging of color fluorescence microscopy (CFM) after Ziel–Neelsen staining. Orange fluorescence (arrows): macrophage foam cells. Arrowhead in γ : residual collagen fibers (CFs). Horizontal bar: 20 μm . A: a plaque without lipids, with abundant normal CFs (a) and without macrophage foam cells (α). B: a plaque with lipids, with thick CFs (b) but without macrophage foam cells (β). C: a plaque with lipid deposition and cavity formation, meager CFs (c) and disseminated macrophage foam cells (arrow in γ). D: a plaque with a thin fibrous cap with lipids and calcium (arrow in D), without CFs (d) and with multiple macrophage foam cells (arrows in δ).
Reproduced from Uchida et al. [34], with permission.

DES than that in BMS [47], probably due to the higher prevalence of neointimal coverage. Awata et al. observed that LST was more frequently observed in sirolimus-eluting stents (SES) than in paclitaxel-eluting stents (PES) (43% vs 19%) at 6 months [48]. They also reported that LST was observed in 31% of patients in the SES group versus 6% of patients in the zotalorimus (ZES) group at 6 months.

Possible mechanisms of late-stent thrombosis and appropriate neointimal thickening to prevent restenosis, and neoendothelial cell damages and consequent late-stent thrombosis

Endothelial cells are highly anti-thrombotic. The same may also be true for neoendothelial cells regenerated after stent implantation.

Neointima acts as a cushion between neoendothelial cells and the stent struts. If the neointima is thin, stent struts are considered to be dislocated synchronizing to blood pressure changes and cardiac motion, and accordingly induce mechanical stress on the neoendothelial cells.

The struts were see-through (grade 0–1) by angioscopy when the neointima thickness was below 130 μm by OCT in patients [49]. LST was observed in grade 0 or 1 group in patients with DES or BMS [10,26,50]. At 6 months after stenting, neoendothelial cells were stained in blue with Evans blue dye which selectively stains damaged endothelial cells when the neointima thickness grade was 0–1 [50,51] (Fig. 11). In animals, the struts were visible (grade 0 or 1) when the neointimal thickness was around 88 μm and LST was frequently observed when the intimal thickness was within 100 μm [51]. All these findings indicated that neoendothelial cells were damaged and LST formed on the

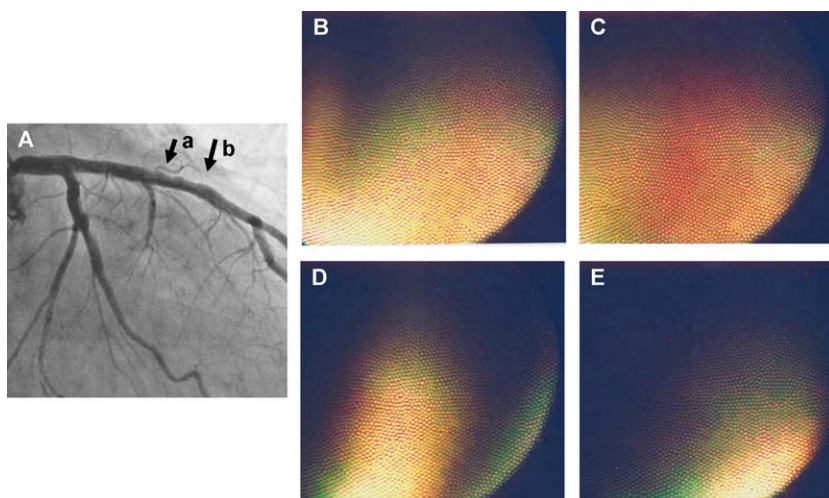


Figure 7 Ox-LDL imaged by color fluorescence angiography (CFA) in the coronary artery in a patient with angina pectoris. Reddish brown fluorescence observed in a non-stenotic proximal segment of the left anterior descending coronary artery after the intra-coronary injection of EB in a patient with stable angina pectoris. A: an angiogram of the left coronary artery. Arrows a to b: the proximal segment observed by CFA. The wall of the segment was uneven but significant stenosis was not found. From B to E: CFA images of the same segment obtained after injecting EB, by advancing the angioscope distally from a to b of panel A. Reddish brown portions indicate ox-LDL. The luminal surface was uneven, indicating early stage of atherosclerosis. Reproduced from Uchida et al. [34] with permission.

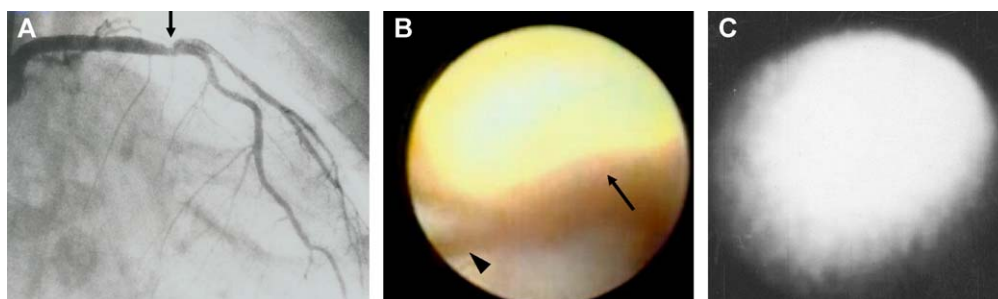


Figure 8 Near-infrared fluorescence angiography (NIRFA) study in a 61-year-old male with stable angina. From A to C: angiogram, conventional angioscopic image and NIRFA image of a plaque in the proximal segment of the left anterior descending coronary artery (arrow in A). The yellow plaque (arrow in B) presented a homogenous type near-infrared fluorescence (NIRF) image (C). Arrowhead: guide wire. Reproduced from Uchida et al. [39], with permission.

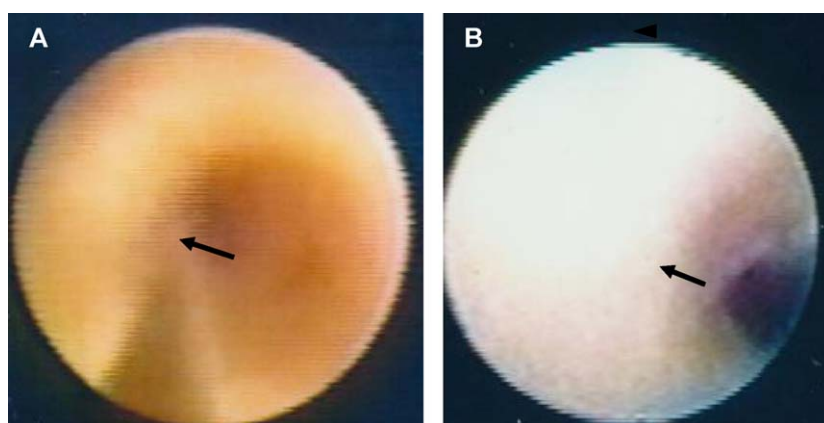


Figure 9 Effects of oral administration of bezafibrate on coronary plaques. A: a yellow plaque before administration of bezafibrate (arrow). B: the yellow plaque (arrow in A) disappeared 6 months later (arrow in B). Reproduced from Uchida et al. [18] with permission.

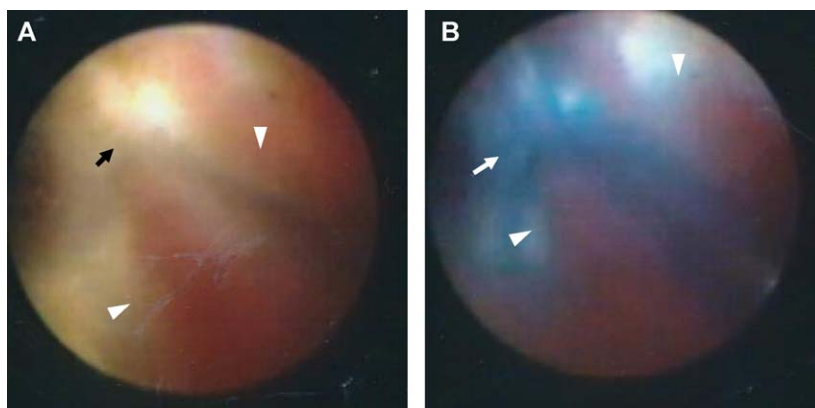


Figure 10 An occlusive stent thrombus (late-stent thrombosis) formed 7 months after bare-metal stent (BMS) deployment. A and B: A 57-year-old-male in whom ST-elevation myocardial infarction developed 7 months after BMS deployment. Arrow in A: naked (grade 0) strut. Arrowheads: occlusive red thrombi. Arrow in B: struts and neighboring portions stained blue with Evans blue indicating neoendothelial cell (NEC) damage and/or fibrin. Arrowheads correspond to those in A.

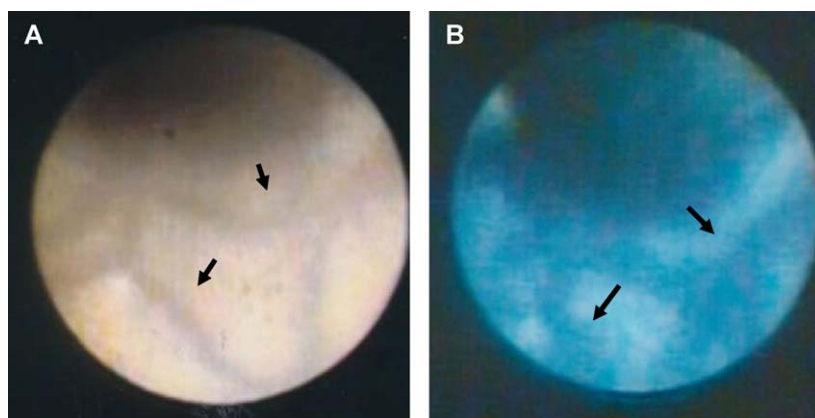


Figure 11 Staining of neoendothelial cells (NECs) 6 months after bare-metal stent (BMS) deployment. Neointimal coverage was grade 1 because the struts were seen through (arrows in A). The struts were stained with Evans blue, indicating neoendothelial cell (NEC) (arrows in B) damage.

struts when neointimal thickness was within approximately 100 μm .

Determining exactly how to terminate this “vicious cycle” is an essential requisite for effective prophylactic treatment of LST.

Based on the angioscopic results in these clinical and animal studies, the control of neointimal regeneration over 100 μm and below an appropriate thickness that does not cause significant restenosis is an essential requisite for the prevention of LST and restenosis.

Conclusion

Dark and glistening yellow coronary plaques observed by conventional angiography using visual light have been believed to be vulnerable based on the studies in patients with ACS, histological examinations, and on prospective studies. Further, the patients having multiple yellow plaques have been believed more prone to suffer from ACS. Why the patients having yellow plaques do not necessarily suffer from ACS is a recently raised question. Based on lipids, collagen fibers, and calcium distribution patterns, yellow

coronary plaques are classified by histology into 7 stable or vulnerable subgroups and conventional angiography can not discriminate them. Recently, new imaging modalities were developed to discriminate the substances or cells that constitute the atherosclerotic plaques, namely near-infrared spectroscopy and fluorescence angiography and so on. Employing these imaging modalities, more specific identification of vulnerable plaques can be attained.

DES reduce coronary restenosis significantly, however, LST occurs, which requires long-term antiplatelet therapy.

Angioscopic grading of neointimal coverage of coronary stent struts has been established, and it was revealed that neointimal formation is incomplete and prevalence of LST is higher in DES when compared to BMS. It was also observed that the neointima is thicker and LST is less frequent in PES and ZES than in SES.

Endothelial cells are highly anti-thrombotic. Clinical and animal studies have revealed that neoendothelial cells on stent struts are damaged when the neointima is less than 100 μm thick, and LST frequently occurs. In addition to toxic effect of drugs or polymers of DES, neoendothelial cell damage is considered to be caused by friction between the cells and stent struts due to the thin neointima between them

which might act as a cushion. Therefore, it is conceivable that to control neointimal regeneration over 100 μm and below appropriate thickness which does not cause significant restenosis is necessary to prevent LST.

References

- [1] Allen DS, Graham EA. Intracardiac surgery: a new method. *Am Med Assoc* 1922;79:1028.
- [2] Uchida Y, Tomaru T, Sumino S, Kato S, Sugimoto T. Fiberoptic observation of thrombosis and thrombolysis in isolated human coronary artery. *Am Heart J* 1986;112:694–6.
- [3] Spears JR, Spokojny AM, Marais HJ. Coronary angiography during cardiac catheterization. *J Am Coll Cardiol* 1985;6:93–7.
- [4] Litvack F, Grundfest WS, Lee ME. Angioscopic visualization of blood vessel interior in animals and humans. *Clin Cardiol* 1985;8:65–70.
- [5] Uchida Y, Nakamura F, Tomaru T, Furuse A, Fujimori Y, Hasegawa K. Percutaneous coronary angiography in patients with ischemic heart disease. *Am Heart J* 1987;114:1216–22.
- [6] Hoeler M, Hombach V, Hoepf HW. Percutaneous coronary angiography during cardiac catheterization. *J Am Coll Cardiol* 1988;11(65A) [abstract].
- [7] Uchida Y, Tomaru T, Sugimoto T. Angioscopic observation of coronary luminal changes induced by PTCA. *Proc Jpn Coll Angiol* 1984;85 [abstract].
- [8] Uchida Y, Hasegawa K, Kawamura K, Shibuya I. Angioscopic observation of the coronary luminal changes induced by percutaneous transluminal coronary angioplasty. *Am Heart J* 1989;117:769–76.
- [9] Nakamura F, Kvasnicka J, Uchida Y, Geschwind HJ. Percutaneous angioscopic evaluation of luminal changes induced by excimer laser angioplasty. *Am Heart J* 1992;124:1467–72.
- [10] Ueda Y, Nanto S, Komamura K, Kodama K. Neointimal coverage of stents in human coronary arteries observed by angiography. *J Am Coll Cardiol* 1994;23:341–6.
- [11] Ishikawa H, Uchida Y. Angioscopic features of coronary artery in Kawasaki disease. In: *Proceedings of 4th international Kawasaki disease conference*. 1991. p. 20–2.
- [12] Sherman CT, Litvack F, Grandest W, Lee M, Hickey A, Chaux R, Blanche C, Matloff J, Morgenstern L. Coronary angiography in patients with unstable angina pectoris. *New Engl J Med* 1986;315:913–9.
- [13] Uchida Y, Fujimori Y, Ohsawa H, Noike H. Angioscopic evaluation of the stabilizing effects of bezafibrate on coronary plaques. *Coronary* 1997;16:293–301.
- [14] Uchida Y, Tomaru T, Sugimoto T. Angioscopic observation of coronary luminal changes induced by PTCA. *Proc Jpn Coll Angiol* 1984;50 [abstract].
- [15] Uchida Y, Nakamura F, Tomaru T, Oshima T, Sasaki T, Morizuki S, Hirose J. Prediction of acute coronary syndromes by percutaneous coronary angiography in patients with stable angina pectoris. *Am Heart J* 1995;130:195–203.
- [16] Uchida Y. *Coronary angiography*. Futura: Armonk, NY; 2001. p. 79–100.
- [17] Ueda Y, Ohtani T, Shimizu M, Hirayama A, Kodama K. Assessment of plaque vulnerability by angioscopic classification of plaque color. *Am Heart J* 2004;148:333–5.
- [18] Uchida Y, Fujimori Y, Ohsawa H, et al. Angioscopic evaluation of stabilizing effects of bezafibrate on coronary plaques in patients with coronary artery disease. *Diag Therap Endosc* 2000;7:21–8.
- [19] Ishibashi F, Mizuno K, Kawamura A, Shin PP, Nesto RW, Waxman S. High yellow color intensity by angiography with quantitative colorimetry to identify high-risk features in culprit lesions of patients with acute coronary syndromes. *Am J Cardiol* 2007;100:1207–11.
- [20] Okada K, Ueda Y, Oyabu J, Ogasawara N, Hirayama A, Kodama K. Plaque color analysis by the conventional yellow-color grading system and quantitative measurement using LCH color space. *J Interv Cardiol* 2007;20:324–34.
- [21] Uchida Y, Egami H. What determines depth of yellow color of coronary plaques. *Proceedings of 20th annual meeting of Japanese Association of Cardioangiography* 2005:15.
- [22] Ohtani T, Ueda Y, Mizoe I, Oyabu J, Okada K, Hirayama A, Kodama K. Number of yellow plaques detected in a coronary artery is associated with future risk of acute coronary syndrome: detection of vulnerable patients by angiography. *J Am Coll Cardiol* 2006;47:2194–200.
- [23] Takano M, Jang IK, Inami S, Yamamoto M, Murakami D, Komatsu K, Seimiya K, Ohba T, Mizuno K. In vivo comparison of optical coherence tomography and angiography for the evaluation of coronary plaque characteristics. *Am J Cardiol* 2008;101:471–6.
- [24] Komatsu S, Ueda Y, Omori Y, Kodama K. Diagnosis of vulnerable plaque and vulnerable patients by coronary angiography and multi-detector row computed tomography (MCDCT)-from invasive to non-invasive plaque imaging. *Vasc Dis Preven* 2006;3:319–25.
- [25] Uchida Y, Egami H, Kameda N. Pitfalls of angiography in detecting vulnerable coronary plaques. *Circ J* 2010;74:273.
- [26] Uchida Y. Angioscopic detection of vulnerable coronary plaques. *Curr Cardiovasc Imag Rep* 2010;3:222–9.
- [27] Stary HC, Chandler AB, Dinsmore RE, Fuster V, Glagov S, Insull Jr W, Rosenfeld ME, Schwarz CJ, Wagner WD, Wissler RW. A definition of advanced types of atherosclerotic lesions and a histological classification of atherosclerosis: a report from the committee on vascular lesions of the council on arteriosclerosis, American Heart Association. *Circulation* 1995;92:1355–74.
- [28] Tavora F, Cresswell N, Li L, Ripple M, Fowler D, Burke A. Sudden coronary death caused by pathologic intimal thickening without atheromatous plaque formation. *Cardiovasc Pathol* 2009;26:55–61.
- [29] Uchida Y, Uchida Y, Sakurai T, Kanai M, Shirai S, Oshima T, Tabata T. Fluffy luminal surface of the non-stenotic culprit coronary artery in patients with acute coronary syndrome. *Circ J* 2010;74:2379–85.
- [30] Romeo F, Li D, Shi M, Mehta JL. Carvedilol prevents epinephrine-induced apoptosis in human coronary artery endothelial cell: modulation of Fas/Fas ligand and caspase-3 pathway. *Cardiovasc Res* 2000;45:788–94.
- [31] Weinmann P, Jouan M, Nguyen QD, Lacroix B, Groiselle C, Bonte JP, Luc G. Quantitative analysis of cholesterol and cholesteryl esters in human atherosclerotic plaques using near-infrared Raman spectroscopy. *Atherosclerosis* 1998;140:81–8.
- [32] Garg R, Waxman S. Catheter-based near-infrared spectroscopy for imaging of lipid-rich plaques. *Curr Cardiovasc Imaging Rep* 2010;3:403–11.
- [33] Uchida Y, Noike H, Tomaru T, Kanai M, Sakurai T. Two-dimensional imaging of lipids deposited in the coronary plaques by near-infrared fluorescence angiography. *Circulation* 2007;118(Suppl. II):617.
- [34] Uchida Y, Uchida Y, Kawai S, Kanamaru R, Sugiyama Y, Tomaru T, Maezawa Y, Kameda N. Detection of vulnerable coronary plaques by color fluorescent angiography. *JACC Cardiovasc Imaging* 2010;3:398–408.
- [35] Halvorsen B, Otterdal K, Dahl TB, Skjelland M, Gullestad L, Oie E, Aukrust P. Atherosclerotic plaque stability—what determines the fate of plaque? *Prog Cardiovasc Dis* 2008;51:183–94.
- [36] Shah PK. Inflammation and plaque vulnerability. *Cardiovasc Drugs Ther* 2009;23:31–40.
- [37] Aiyar N, Disa J, Ao Z, Ju H, Nerurkar S, Willette RN, Macphee CH, Johns DG, Dougl SA. Lysophosphatidylcholine induces inflammatory activation of human coronary artery smooth muscle cells. *Mol Cell Biochem* 2007;295:113–20.

- [38] Uchida Y, Uchida Y, Kawai S, Kanamaru R, Kameda N. Imaging of lysophosphatidylcholine in human coronary plaques by color fluorescence angiography. *Int Heart J* 2010;51:129–33.
- [39] Uchida Y, Uchida Y, Sugiyama Y, Kanai M, Sakurai T, Shirai S. Two-dimensional visualization of cholesterol and cholesteryl esters within human coronary plaques by near-infrared fluorescent angiography. *Clin Cardiol* 2010;33:322–5.
- [40] Takano M, Mizuno K, Yokoyama S, et al. Changes in coronary plaque color and morphology by lipid-lowering therapy with atorvastatin: serial evaluation by coronary angiography. *J Am Coll Cardiol* 2003;42:680–6.
- [41] Hirayama A, Saito S, Ueda N, Takayama T, Honye J, Komatsu S. Effects of strong statin on the stabilization and regression of coronary plaques as evaluated by coronary angiography and intravascular ultrasound in Japanese subjects-TWINS and TOGETHAR study. *Circ J* 2010;73:718–25.
- [42] Higo T, Ueda Y, Oyabu J, Okada K, Nishio M, Hirata A, Kashiwase K, Ogasawara N, Hirotsu S, Kodama K. Atherosclerotic and thrombogenic neointima formed over SES. *JACC Cardiovasc Imaging* 2009;2:616–24.
- [43] Oyabu J, Ueda Y, Ogasawara N, Okada K, Hirayama A, Kodama K. Angiographic evaluation of neointimal coverage: sirolimus drug-eluting stent versus bare metal stent. *Am Heart J* 2006;52:1168–74.
- [44] Sakai S, Mizuno K, Yokoyama S, Tanabe J, Shinada T, Seimiya K, Takano M, Ohba T, Tomimura M, Uemura R, Imaizumi T. Morphologic changes in infarct-related plaque after coronary stent placement. *J Am Coll Cardiol* 2003;42:1558–65.
- [45] Awata M, Kotani J, Uematsu M, Morozumi T, Watanabe T, Onishi T, Iida O, Sera F, Nanto S, Hori M, Nagata S. Serial angiographic evidence of incomplete neointimal coverage after SES implantation. *Circulation* 2007;116:910–6.
- [46] Awata M, Nanto S, Uematsu M, Morozumi T, Watanabe T, Onishi T, Sera F, Kotani J, Hori M, Nagata S. Angiographic comparison of neointimal coverage between zotarolimus- and sirolimus-eluting stents. *J Am Coll Cardiol* 2008;52:789–90.
- [47] Takano M, Ohba T, Inami S, Seimiya K, Sakai S, Mizuno K. Angiographic differences in neointimal coverage and in persistence of thrombus between sirolimus-eluting stents and bare-metal stents after 6-month implantation. *Eur Heart J* 2006;27:2189–95.
- [48] Awata M, Nanto S, Uematsu M, Morozumi T, Watanabe T, Onishi T, Iida O, Sera F, Minamiguchi H, Kotani J, Nagata S. Heterogeneous arterial healing in patients following paclitaxel-eluting stent implantation. *J Am Coll Cardiol Interv* 2009;2:453–8.
- [49] Tsujimoto T. Relationships between angiographic images of coronary stents and neointimal thickness measured by OCT. Proceedings of the 20th annual meeting of the Japanese Cardioangiography Society 2006:30.
- [50] Uchida Y, Uchida Y, Fujimori Y. Endothelial cells covering coronary stents are frequently damaged. *Circulation* 2006;114(Suppl. II):591.
- [51] Uchida Y, Uchida Y, Sakurai T, Kanai M. Possible role of damaged neo-endothelial cells in the genesis of coronary stent thrombosis: a dye-staining angiographic study. *Int Heart J* 2010;51:700–6.